

1. Urszula NAWROT<sup>1</sup>, 2. Mikołaj DEMUTH<sup>1</sup>, 3. Andrzej SIERAKOWSKI<sup>2</sup>, 4. Ewelina GACKA<sup>1</sup>,  
5. Krzysztof PAŁKA<sup>3</sup>, 6. Teodor GOTSZALK<sup>1</sup>

Wrocław University of Science and Technology, Department of Nanometrology (1), Łukasiewicz Research Network, Institute of Microelectronics and Photonics (2) Nanores - Nano Science and Technology Institute (3)

ORCID: 1. 0000-0002-7207-5680; 2. 0009-0002-5151-328X, 3. 0000-0002-5482-5812, 4. 0009-0004-9788-7345, 5. 0000-0003-4182-9192

doi:10.15199/48.2023.10.01

## Overview of light coupling methods to optical planar waveguides

**Abstract.** Due to the growing demands on the speed and amount of data transmission, more and more researchers worldwide are looking for a replacement medium for information transmission. An alternative to standard electronics is integrated optics. However, it is not on the level of development to be used on a large scale. One of the problems is the efficient coupling of the light into integrated structures. This study presents two ways to couple light into such structures and what aspects should be considered when selecting one of these methods.

**Streszczenie.** Ze względu na rosnące wymagania dotyczące szybkości i ilości przesyłanych danych, coraz więcej badaczy na całym świecie poszukuje zastępczego medium do transmisji informacji. Alternatywą dla standardowej elektroniki jest zintegrowana optyka. Nie jest ona jednak na takim poziomie rozwoju, by mogła być wykorzystywana na szeroką skalę. Jednym z problemów jest efektywne sprzężenie światła w zintegrowanych strukturach. W niniejszym artykule przedstawiono dwa sposoby wprowadzania światła do takich struktur oraz aspekty, które należy wziąć pod uwagę przy wyborze jednej z tych metod. (Przeгляд метод sprzężenia света з оптычными фалодами планарными)

**Słowa kluczowe:** światłowody planarne, optyka zintegrowana, czujniki światłowodowe.

**Keywords:** optical planar waveguide, integrated optics, optical fiber sensors.

### Introduction

Nowadays, electronics have become an indispensable part of people's daily lives. The rapid development of the semiconductor industry and the miniaturization that has progressed with it have demonstrated significant limitations of the widely spread silicon technology. Quantum effects occurring for nanometer-sized electronic component structures influence their applicability and scalability.

Today, researchers worldwide are looking to change the medium of information transmission. A novel approach involves manufacturing integrated optical and electronic circuits. Fiber-optic technology used primarily for information transmission can also provide an alternative to classical metallic connections and electronic sensors. In long-distance telecommunications, fiber optics with cylindrical geometry made of silica are usually used for the propagation of the light beam signal. An essential problem of integrating such a solution is how to scale the communication optics. There has been an increased interest in optical planar waveguides due to their very small size, even compared to fiber optics [1]. Integration of optical interconnects (optical fibers) and electronic components (lasers, light detectors), which forms a single structure opens new possibilities for creating superfast combinational systems with almost unlimited transmission bandwidth (over a wide range of optical wavelengths) [2]. The speed of such solutions significantly exceeds current copper-based interconnections used in integrated circuits (ICs) and makes it possible to design multifunctional chemical and biological sensors [3]. An additional advantage of optical sensors is their complete insensitivity to electromagnetic interference stemming from widely used wireless (network) technology, which significantly increases the reliability of such structures compared to electronic sensors.

The relevance of planar optical waveguides in sensor solutions is explained by the possibility of creating asymmetric structures characterized by different refractive indices of the lower and upper cladding (see Fig. 1) [4-6]. By taking the material/ substrate under test as the upper cladding, it is possible to make the sensor sensitive to it. Changes in the refractive index of the upper layer lead to changes in the parameters of the propagated light beam. Then, the appropriate selection of the measured optical quantity (associated with the propagated wave) is the reason for recording the changes and detection.

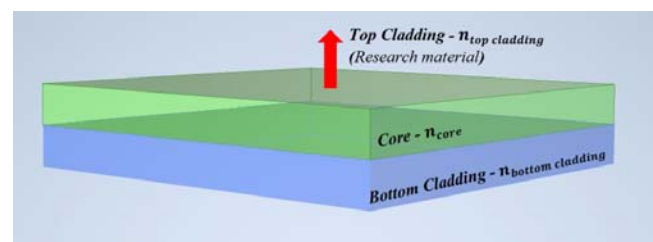


Fig. 1. Asymmetrical optical fiber where the tested material/ substrate acts as the upper cladding

One of the most difficult problems which must be solved by the labs working on the field of optical sensors is how to couple the light beam into the structure. The diameter of the cores of the smallest fiber optics in use is about 9  $\mu\text{m}$ , while the thickness of a planar core is usually less than 1  $\mu\text{m}$ . In extreme cases, the core structure has a thickness less than the wavelength of propagated light. Moreover, the developed solution should ensure not only the precision of the fiber placement but also the durability of the component connection. The current trend indicates the four most popular specialized solutions for introducing light into the planar core of an optical waveguide [7-8]:

- end coupling,
- prismatic coupling,
- coupling with a diffraction grating,
- coupling using a fiber optic taper.

The first two methods mentioned above will be described in detail later in the article. The third method applies a diffraction grating which introduces a periodic change in the refractive index near the core of the optical fiber [9]. Integration of a diffraction grating into the core structure of an optical planar waveguide must be considered already at the design stage of the structure. It is usually fabricated using the same material as the core of the optical fiber. Light is coupled on the top layer of the structure (on the side of the top cladding where the diffraction grating was implemented). Bragg's condition is taken as the condition for introducing light into the structure when designing the coupling grating. Choosing the appropriate refractive angle, deflection order, and wavelength makes it possible to design such a coupler for any structure.

The last method for light coupling is based on the usage of a taper to expand the dimensions of the planar core structure to match the diameter of the optical fiber core. [10]. It is usually fabricated in a single process from the same material as the planar waveguide core or with a similar refractive index as the core. The taper focuses the beam in a core with smaller cross-sectional dimensions and adapts it to the shape of the core. The taper can also be used to widen the light beam to match the fiber optics and to bring the beam out of the integrated optics systems.

A semiconductor light source (i.e., edge emitting lasers) can also be integrated in a single planar waveguide structure. Such a solution allows precise alignment of the light beam source and structure at the design stage [11]. However, the thickness of the emitting structure should be comparable to the core of the planar optical fiber. Ideally, the two structures should be fabricated on the same surface to avoid alignment of them. The high cost of such a solution and the complexity of the production process requires spending much time optimizing it.

Another important aspect of the efficient light guiding into the planar structures is maximizing the optical power propagating in the fiber core. The demand for a given power level can be explained by the optical power detectors that are currently used. The sensitivity of the detectors used in communications ranges from a few to several tens of dBm, depending on the type of design [12]. This aspect is directly related to the light coupling efficiency into the optical planar waveguides.

### Specification of tested the optical planar waveguide

This study aims to characterize samples of optical planar waveguide of the different core lengths from the optical point of view. The planar waveguides were designed to work with a wavelength of light of 635 nm. This experiment makes it possible to test the efficiency of the beam coupling into the previously fabricated planar structure. The tested planar optical waveguides are asymmetric fibers, which means that the refractive index of the top cladding is not equal to that of the bottom cladding. The bottom cladding was made of silicon dioxide ( $\text{SiO}_2$ ) with a refractive index of 1.457 (for a wavelength of 635 nm). The core consists of a thin layer of silicon nitride ( $\text{Si}_3\text{N}_4$ ), which has a refractive index of 2.0102 (corresponding to the wavelength of 635 nm) [13]. The top cladding is formed by the material surrounding the core of the planar optical fiber. It can be, for example, air ( $n = 1$ ), an immersion liquid ( $n = 1.515$ ), or another material placed directly on the core with lower refractive index than the refractive index of the core

material. Thickness of the individual layers of the tested optical planar waveguide was:

- substrate, Si: 400  $\mu\text{m}$ ,
- bottom cladding, ( $\text{SiO}_2$ ): 1  $\mu\text{m}$ ,
- core, ( $\text{Si}_3\text{N}_4$ ): 0.33  $\mu\text{m}$ ,
- top cladding: the thickness of applied medium/air.

Three structures with different core lengths of the planar waveguides are available: 4 mm, 7 mm, and 10 mm (see Fig. 2). Each planar optical fiber has a width of the order of 1 cm. V-grooves have been made in the structures to make it easier to insert the light using the end coupling method with the optical fiber (see Fig. 3). The optical fibers can be pasted with a specialized adhesive and integrated into the entire planar waveguide structure.

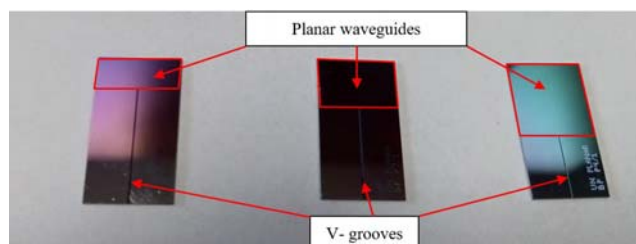


Fig. 2. Planar waveguides in lengths: 4 mm, 7 mm and 10 mm

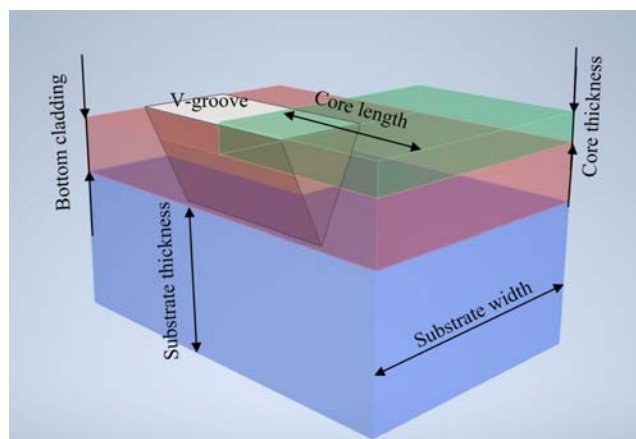


Fig. 3. Scheme of the tested planar optical fiber – the drawing is not in scale

### Fabrication process of the optical planar waveguide

The structure was fabricated by the Institute of Microelectronics and Photonics in Warsaw. The doubly side polished (DSP) silicon 4" wafers with {100} crystallographic orientation, n-type conductivity was used as a start substrate. The entire fabrication process is divided into three main steps.

In the first step 40nm thick silicon nitride was deposited on a silicon wafer in the LPCVD (Low-Pressure Chemical Vapor Deposition) process. Next, the mask in silicon nitride, defining the V-grooves shape, was prepared in plasma etching following a photolithography process. The goal was to manufacture the V-groove, which should be used to position the optical fiber in such a way that its core is at the height of the upper plane of the structure (see Fig. 4).

In the opened windows KOH etching will be stopped by {111} planes at the edge of the pattern. As the result V-groove depressions are formed, in which the angle of inclination of the walls relative to the upper plane results directly from the properties of the silicon crystal and is 54.74°. The analysis of the geometric relationships allows for the determination of the window whose width was defined in the photolithography process.

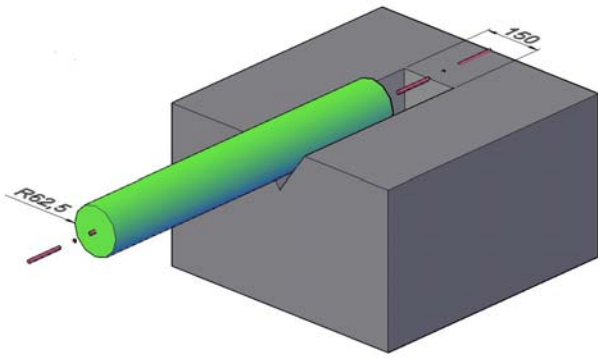


Fig. 4. 3-D model - optical fiber positioned in V-groove (design assumptions)

To sum up, to place a fiber of  $125\ \mu\text{m}$  in a V-groove in the way the fiber core is at the height of the upper structure plane, the lithographically defined width of the V-groove should be  $150\ \mu\text{m}$ .

In the second step, the KOH wet etching process was used to form the V-grooves on the surface of the silicon wafer. Next, the silicon nitride mask was removed. In the third step, target dielectric layers were defined. Firstly, a  $1\ \mu\text{m}$  thick silicon dioxide was thermally grown in a wet oxidation process. Next, the LPCVD process was applied to deposit a  $330\ \text{nm}$  thick silicon nitride layer (see Fig. 5).

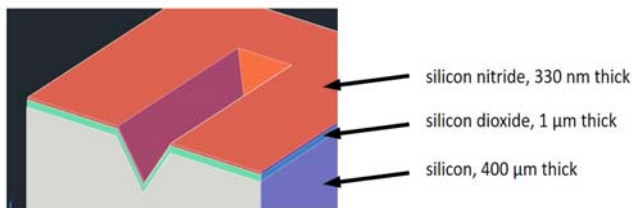


Fig. 5 V-groove structure for the placement of the optical fibers

### Light coupling from an optical fiber to an optical planar waveguide

In order to achieve the coupling of light from an optical fiber to a planar waveguide, there must be direct contact between their front surfaces. The front surface of the planar waveguide must be smooth, and the light must be introduced within the acceptance cone.

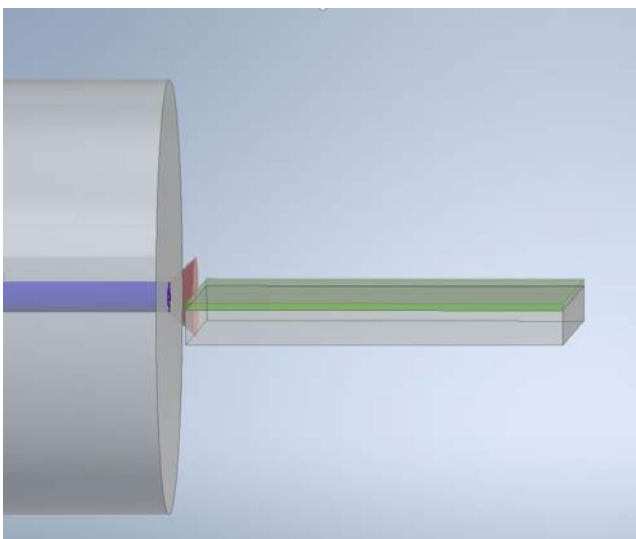


Fig. 6. Scheme of light coupling to a planar optical waveguide from an optical fiber- the drawing is not in scale

Coupling light from an optical fiber into a planar waveguide is difficult because of the required submicron precision in the positioning of the faces of the optical cores relative to each other. When the core of an optical fiber protrudes, its front surface above the core of a planar waveguide, the light will also propagate in the top cladding or, for the asymmetric optical fibers, in the medium surrounding the core, e.g. air (see Fig. 6). The beam's divergence exiting the optical fiber propagates over the surface of the asymmetric planar optical fiber and becomes an essential issue in measuring the output optical power. Divergence is the growth of the cross-sectional diameter of the light beam with increasing distance from the source. It will cause the detector surface to be covered mainly by the beam coming from the light source. As the result, the measured optical power will depend on the light being propagated in the core of the planar waveguide and above it.

A phenomenon that makes it difficult to determine whether light is propagating in the core of a planar waveguide is the diffraction. The layers of the planar waveguides are very thin (on the order of tens of nanometers), which means that a beam reaching the edge of a planar waveguide can be diffracted. In such a case, proving that the zero-order beam comes from the light being propagated in the planar waveguide core is difficult. The method also requires specialized instrumentation to position the end of the optical fiber to the plane of the planar waveguide.

In our investigations the experimental setup consisted of a semiconductor laser diode (Thorlabs S1FC635 at  $635\ \text{nm}$ ), an optical fiber (FiberTechnic FC/UPC 1m single-mode pigtail), attachment of an optic fiber (customized polymer strip  $5\ \text{mm}$  thick with pasted thermopad and made stabilizing holes for screwing to the position meter), a planar optical fiber, a stepper motor (Thorlabs MAX343 - 3-Axis NanoMax Stage and Thorlabs RB13P1/M table), stepper motor controller (Thorlabs BSC103 - Three-Channel APT S/N 70825568) and a detector with an optical power meter (Ophir Orion P/N:7Z01806 with measurement head up to  $1000\ \text{nm}$ ) (see Fig. 7). The optical fiber was glued to a transparent beam and was the stationary element of the system relative to which the planar structure was positioned in the x, y, and z axes. The goal was to place the fiber cores so that the light would not propagate over the top layer of the planar structure.

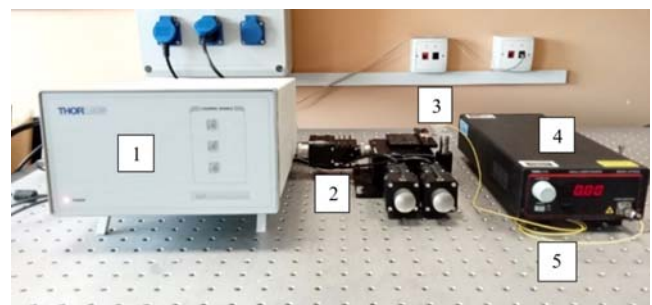


Fig. 7. Measurement setup 1) stepper motor controller, 2) ThorLabs MAX343 - 3-Axis NanoMax Stepper Motors, 3) sample placed on stabilizing beams, 4) pigtail, 5) semiconductor laser -  $635\ \text{nm}$

The thickness of the planar waveguide core ( $330\ \text{nm}$ ) is much smaller than the diameter of the optical fiber used ( $9\ \mu\text{m}$ ). Determination of the area of the planar optical fiber overlapping the area of the optical fiber core is possible to estimate how much optical power will be coupled to the planar structure. The determined area of the planar waveguide is a slice of a circle - its upper edge is the tangent to the perimeter of the fiber optic core (see Fig. 8).

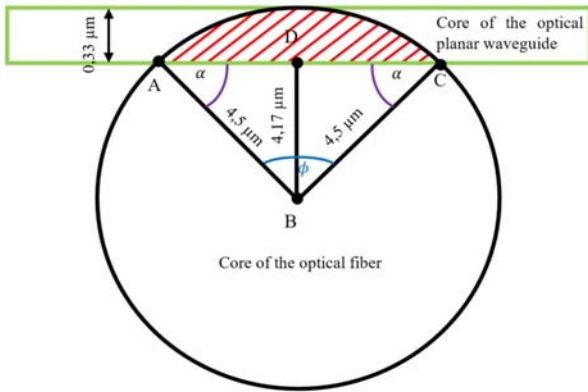


Fig. 8. Illustration of the calculations performed to determine the plane of the faces of the cores that overlapped - the area hatched in red is the calculated area

After making the appropriate calculations and assuming the simplification that the output power from the face of the fiber optic fiber core is distributed uniformly over the entire surface of the optical fiber, the input power of the planar waveguide can be estimated. The power coupled to the planar structure will be ca. 1.2% of the total power propagated in the optical fiber. This value represents the theoretical light coupling efficiency from the single-mode optical fiber to the optical planar waveguide. In practice, it can be much lower due to coupling losses and the transition of the light beam from a material with a lower refractive index (a fiber optic fiber made of silica,  $n=1.45$ ) to a medium with a higher refractive index ( $\text{Si}_3\text{N}_4$ ,  $n=2.01$ ). From the optical power measured at the end of the single-mode optical fiber, it is possible to determine the power introduced into the planar fiber by multiplying it by the calculated coupling efficiency (Tab. 1.).

Table 1 Optical power measurement table of measurements made using the end coupling method for optical planar waveguide

	$P_{\text{fiber}}$	$P_{\text{in}}$ ( $P_{\text{fiber}} \cdot 1,16\%$ )	$P_{2\text{-out}}$	$P_{1\text{-out}}$
Lp.				
1.	131,64	1,53	0,16	1,05
2.	275,34	3,19	0,34	2,19
3.	436,34	5,06	0,54	3,45
4.	591,34	6,86	0,71	4,72
5.	753,34	8,74	0,85	6,04
6.	915,34	10,62	1,25	6,91
7.	1072,34	12,44	1,47	8,24
8.	1236,34	14,34	1,60	9,48
9.	1395,34	16,19	2,05	10,73
10.	1568,34	18,19	2,27	11,97
11.	1733,34	20,11	2,49	13,34
12.	1896,34	22,00	2,68	14,66
13.	2065,34	23,96	2,82	16,01
14.	2225,34	25,81	2,93	17,04
15.	2385,34	27,67	3,64	18,40
16.	2555,34	29,64	3,91	19,33

Fig. 9 represents a correlation of the input power (injected into the optical planar waveguide) to the output power in this waveguide. Since it was difficult to determine the exact position of the two fibers relative to each other (despite using a digital microscope), measurements were made for two positions of the planar waveguide relative to the optical fiber ( $P_{1\text{-out}}$ ,  $P_{2\text{-out}}$ ). From the results, calculations were carried out to determine the attenuation coefficient ( $\alpha$ ) for an optical planar waveguide with a length of 1 cm. The attenuation coefficient for the maximum power in the first position was  $-9.34$  dB/cm, while in the second position, it was  $-1.75$  dB/cm. However, it should be remembered, that

the value taken as the input power is the value measured on the optical fiber and multiplied by the percentage that the planar fiber overlaps with the fiber optic fiber. Hence, it is difficult to calculate the reliable value of attenuation coefficient for this method. The differences in the results of these calculations indicate that some of the light may have partially propagated over the core.

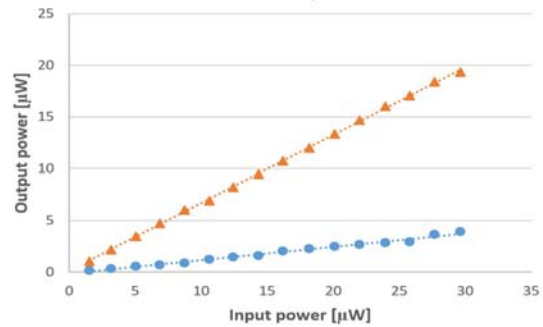


Fig. 9. Graph showing output and input optical power values for optical planar waveguide

### Light coupling from an optical fiber to an optical planar waveguide using V-grooves

The coupling method from an optical fiber to an optical planar waveguide with dedicated V-grooves is based on the same assumptions. The only difference is a positioning of an optical fiber regarding the optical planar waveguide. The advantage of this solution is that integrating the faces of the fiber cores in the case of adequately selected V-groove depth should be better than in the end coupling method. The V-groove avoids the process of long-term positioning of the fiber optic faces relative to each other and makes the system independent of the accuracy of positioning instruments. The position height of the optical fiber is primarily defined in the design of the planar waveguide, and it depends on how deep the V-groove is.

Due to the anisotropic wet etching of the silicon at  $54.7^\circ$ , post-processing of the planar waveguide samples was needed to allow the preparation of a perpendicular end of the V-groove, to which the end surface of the optical fiber would be aligned. A scanning electron microscope (SEM) with gallium-focused ion beam (Ga-FIB) Helios Nanolab 600i was used. Local modifications of the samples using the ion beam with a resolution of tens of nanometres can be performed with the system. The main functions of the FIB microscope, in addition to imaging, are material deposition using a gas injection system [14], milling [15], and ions implantation into the sample material [16]. The SEM with FIB Helios Nanolab 600i applies a Ga-FIB with a current in the  $1.1$  pA -  $65$  nA range and an accelerating voltage from  $500$  V to  $30$  kV. By increasing the Ga-FIB accelerating voltage, the penetration depth of ions into the material is deeper. The value of the FIB current affects the milling speed. Typically, a higher FIB current is used to mill larger volumes, while a low current is applied to mill small shapes with well-defined feature mapping. Considering the height and width of the V-channel used to align the fiber optics with respect to the planar waveguide equal to  $120$   $\mu\text{m}$  and  $155$   $\mu\text{m}$ , respectively, the Ga-FIB parameters of  $30$  kV and  $65$  nA were first used to mill the end surface. Then, in order to eliminate the resulting curtain effect and artifacts on the front surface, gentle milling was performed with a Ga-FIB with a lower current of  $0.79$  nA (see Fig. 10 – Fig. 12). However, due to the long duration of processing with this method (4h), it was decided to perform processing with a femtosecond laser. This process was carried out by an external company, Nanores.

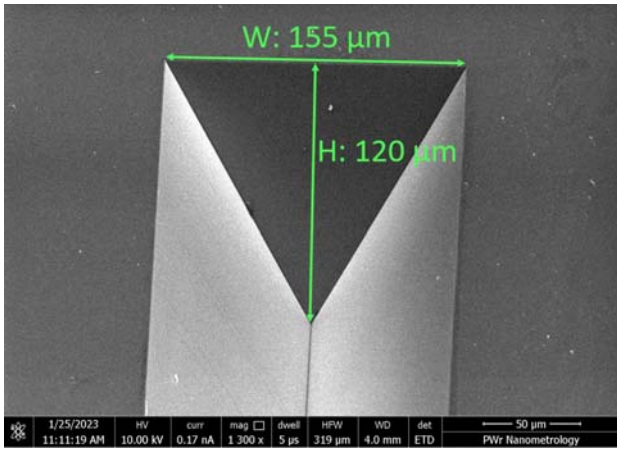


Fig. 10. Scanning electron microscopy (SEM) image of the V-groove end before the milling process (image taken with the tilted SEM stage)

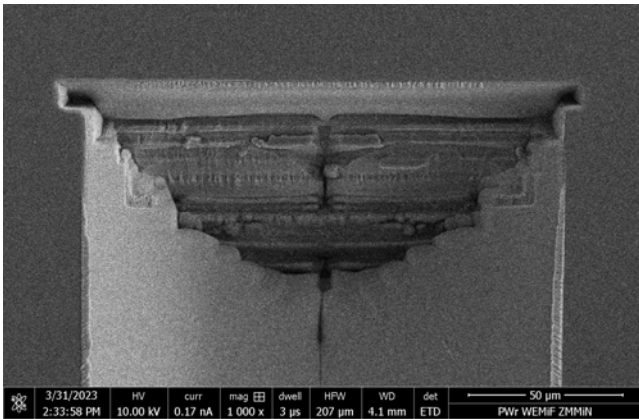


Fig. 11. Scanning electron microscopy (SEM) image of the V-groove end during the milling process (top view)

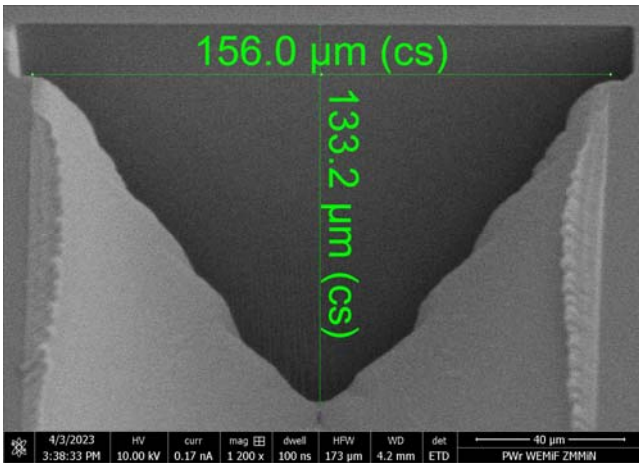


Fig. 12. Scanning electron microscopy (SEM) image of the V-groove end after the milling process (image taken with the tilted SEM stage)

The system used consisted of a Jasper 30- a laser pulse source emitting 1030nm 230fs pulses, PrecSYS 1030 – 5 axis beam positioning system focusing the beam into 16 $\mu$ m spot and XYZ sample positioning system -PIGlide XY motion stage with an OptoSigma OSMS40-5ZF Z motion stage. Correction of the V-groove was done by laser ablation. It involved vaporizing the excess silicon layer along with a "bevel" that prevents direct contact between the faces of the fiber cores. All three samples have been successfully machined. One of them showed cracks in the surface layer.

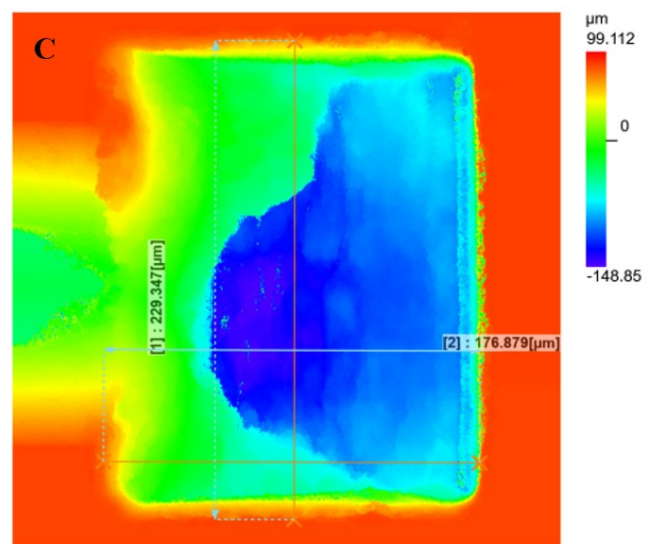
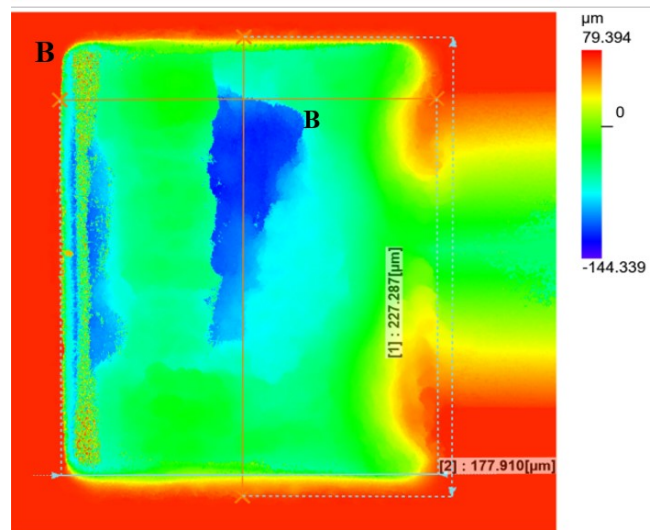
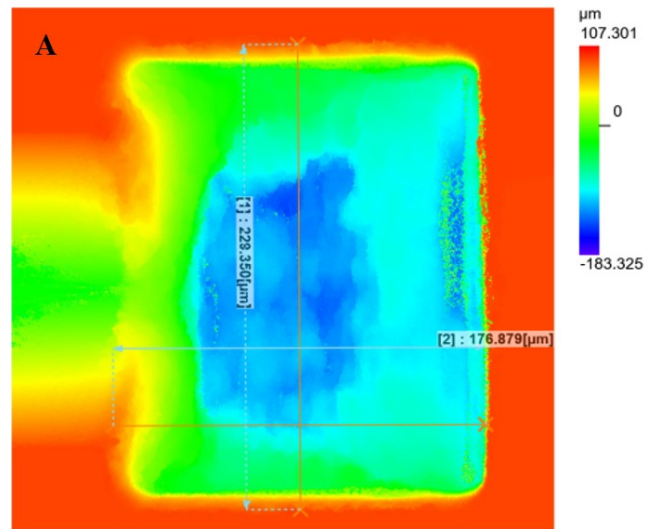


Fig. 13. The results of modified V-groove ending structure for the optical planar waveguides with lengths: A) 3mm, B) 7mm, C) 10mm

The main challenge during machining was dealing with material redeposition, which showed a sponge-like layer around the machined area. The redeposition bonded too strongly to the base material to be removed by an ultrasonic bath and, due to the small dimensions, could not have been removed by wiping the surface manually. Each area had to be machined in multiple passes to clean the resulting redeposition. Some of the redeposition is also aggregated

in the unmachined part of the groove. To achieve a vertical wall, the beam angle had to be adjusted to  $2,5^\circ$  to compensate for a laser beam divergence. Additionally, pulse energy had to be substantially increased (around 5x increase relative to flat machining material) to achieve fluence high enough to overcome the ablation threshold on a tilted surface. The increased energy could have been one of the reasons for the cracks appearing in one of the samples.

The dimensions and quality of the conducted modifications were examined using an Olympus OLS5100 microscope. The fabricated modifications of the V-groove termination structures were characterized by similar dimensions of a width of about  $229\ \mu\text{m}$  and a length of about  $177\ \mu\text{m}$  (Figure 13). The base of the fabricated cuboid was not perfectly smooth. The Olympus OLS5100 microscope also allowed us to determine the profile of the etched structure. Analyzing the data in Fig. 13, one can see inhomogeneities in the base of the cuboid due to its fabrication method, which involves spot-heating the material to its evaporation temperature. The green color indicates the depth of the V-groove termination. Thus, it can be assumed that the  $0\ \mu\text{m}$  level (corresponding to the green color), marked on the diagram, is the reference value against which the profile of the base of the cuboid was determined. Shades of blue show all the hollows created by the laser ablation process. Modification with the laser allowed faster modification of the groove surface and close adhesion of the fiber core face to the planar core face.

The procedure for preparing specimens for gluing the optical fiber into the V-groove was to mount the planar waveguide on a thermopad and the structure's stiffening beam. This action was intended to prevent an optical fiber from breaking. The optical fiber was positioned in the V-groove relative to the face of the planar waveguide core using a digital microscope so that their faces were in direct contact. A layer of NOA81 adhesive was then applied and exposed to a UV lamp until it became solid. Eventually, a structure could be directly connected to a laser diode via an FC/PC connector (see Fig.14).

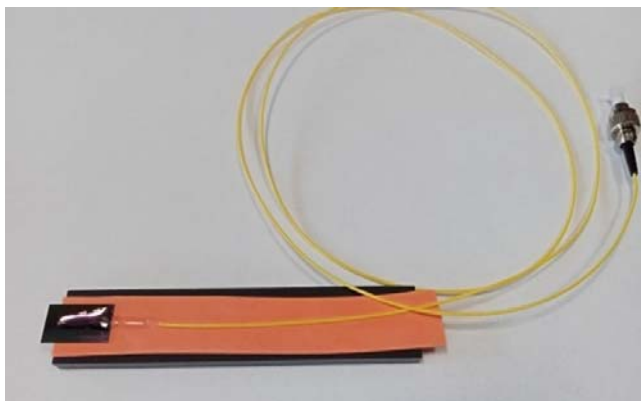


Fig. 14. Optical planar waveguide with embedded optical fiber in the V-groove

Optical microscope (Leica dm 2700m) examinations were performed after the optical fibers were glued into the V-grooves. It was found that for the 4 mm long planar optical fiber structure, the faces of the cores are not in direct contact. It is due to inaccurate positioning of the fiber optic in the V-groove (see Fig. 15). The adhesive probably got between the faces of the cores while curing it, even though the procedure was performed very thoroughly under a digital microscope.

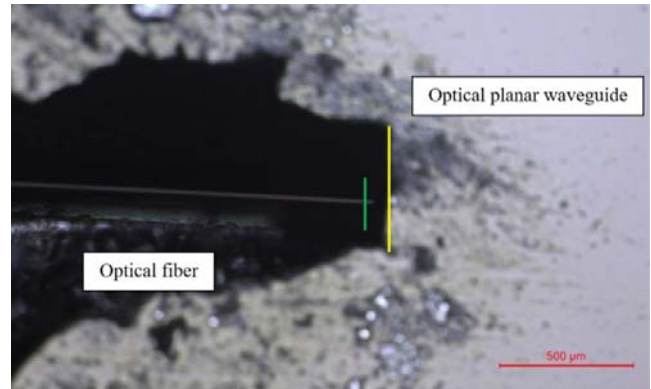


Fig. 15. Optical microscope photo of the interface between the optical fiber and optical planar waveguide fronts (the length of the planar waveguide was 4mm) - the green line corresponds to the end of an optical fiber, and the yellow line corresponds to the beginning of a planar waveguide

In the case of a structure with a 7-mm-long core, it can be concluded that the cores remain in direct contact (see Fig. 16). The black surface on the right side of the contact of the fiber's fronts is glue. It was confirmed by checking the focus at which it occurred.

After applying black to the adhesive and the protruding part of the fiber optic core to prevent light propagation over the planar fiber optic core surface, no light propagation was observed in the structure. In the case of the 4-millimeter-long optical fiber, this is due to the lack of direct contact between the two fiber faces. In contrast, the lack of propagation at a length of 7 mm is likely due to the high attenuation of the structure. Calculations of the structure's attenuation coefficients were also made for the prismatic method, which is described in the next section and is the most efficient method of those tested so far.

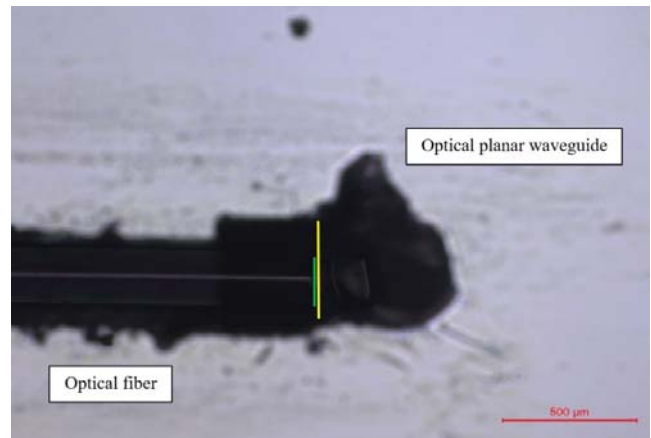


Fig. 16. Optical microscope photo of the interface between the optical fiber and optical planar waveguide fronts (the length of the planar waveguide was 7mm) - the green line corresponds to the end of an optical fiber, and the yellow line corresponds to the beginning of a planar waveguide

#### Coupling from an optical fiber to an optical planar waveguide using a prism

The prism method uses optical prisms to couple the light into a planar waveguide. An interesting aspect of this solution is the complete reversibility of the process, which means that the beam light introduced into the waveguide can also be decoupled from it with a second prism. It is distinguished from the end coupling method by the plane through which the light is coupled into the structure. The prism is placed directly on a layer of the upper cladding,

usually referred to as an air gap - since the upper cladding is usually the air. A beam of light coupled into the prism through the counter prism edge at the appropriate angle is internally reflected on the plane bordering the optical fiber. The coupling of light through an optical prism requires a phase-matching condition. The propagation constant of an optical fiber ( $\beta$ ) determines the change in the parameters of a wave of a particular frequency, amplitude, and phase in the direction of its propagation (1) [11]:

$$(1) \quad \beta = nk_0 \sin \Theta$$

where:  $n$  – refractive index of the medium in which the wave propagates,  $k_0$  – phase constant,  $\Theta$  – angle of reflection of the light beam.

Using the prism method, the propagation constant of the core ( $\beta_c$ ) must be equal to the propagation constant of the prism ( $\beta_{pr}$ ) (see Fig. 17) (2) [11]:

$$(2) \quad \beta_c = n_c k_0 \sin \Theta_c = n_{pr} k_0 \sin \Theta_{pr} = \beta_{pr}$$

In order to meet the above condition, the refractive index of the prism is required to be greater than or equal to the effective refractive index of the optical fiber  $n_{eff}$  (between the bottom cladding and the core) [11] (3).

$$(3) \quad n_{pr} \geq n_{eff}$$

The electromagnetic wave coupled into the prism must meet the conditions of the phenomenon of total internal reflection at the boundary of the prism and the planar waveguide. Due to the overlap of the incident and reflected beam near the optical fiber, a standing wave is formed. Part of the standing wave disappears and, as a result, is coupled into the optical waveguide [1].

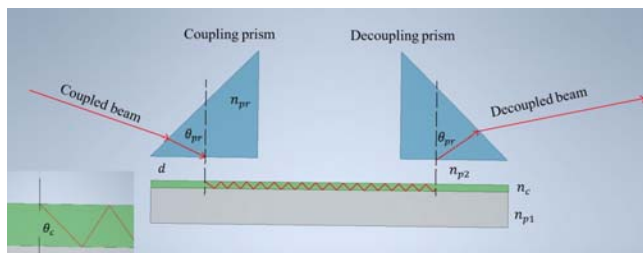


Fig. 17. Schematic a prismatic coupling of light beam into planar waveguide structure - figure is not to scale (based on [8])

To couple light into the structure of a planar waveguide by the prism method, a unique table was designed and built to allow the specimen to be fixed vertically and the angles at which the light beam is introduced into the prism to be observed. In addition, a ruler was placed on it to study the length of the optical fiber over which propagation occurs (the distance from the insertion point to the exit of the optical fiber). The beam from the semiconductor laser (635 nm) was guided through an optical fiber. Then, by appropriately tilting the table, the angle of the beam was changed, looking for one that allows the optical power to enter the planar structure. Changes in optical power were observed with an Ophir Orion detector. The angle-adjustable table has been equipped with a planar light guide mount (thermopad) for quick and safe change of the test sample. A protractor has been placed on the table for easier adjustment of the light beam insertion angle. The ruler allows for measuring the length of the propagated beam in the planar waveguide from the point of insertion to the point of exit from the fiber (see Fig. 18)

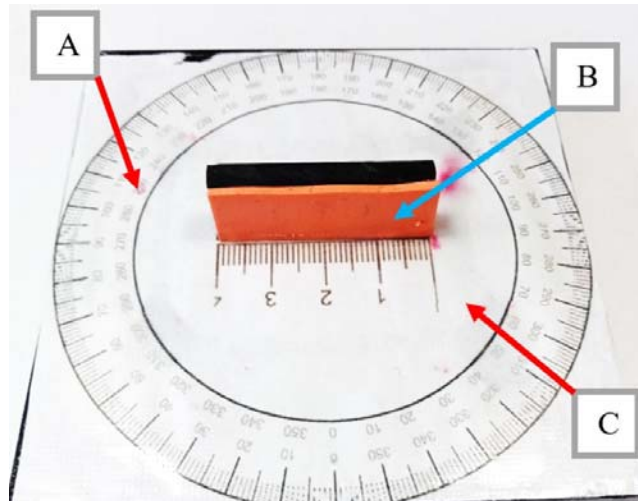


Fig. 18. A table for coupling light into a planar waveguide using the prismatic method: A) protractor, B) thermopad, C) ruler

The measurements include coupling a beam of the light on a given section of planar optical fiber (with a length of 1 cm). As a result, it was possible to carry out measurements not only for the defined sections of the fabricated structures (4 mm, 7 mm, and 10 mm ) but also for any length values between 3 - 10 mm (see Fig. 19 and Fig. 20). . For example, taking as input power the power propagated for the length of the optical fiber 4 mm and as output power the power propagated on a section of 7 mm, it is possible to determine the attenuation coefficient from a 3 mm propagation section. With this solution, the input and output power can be determined unambiguously without estimating the coupling efficiency.

A beam of light coupled into the prism at a suitable angle is refracted and falls on its surface parallel to the core of the planar waveguide. Then, due to the phenomenon of total internal reflection, the beam is reflected from this surface. As a result of the interaction of the reflected and incident beam with each other, a standing wave is formed. The evanescent field of this wave is coupled into the structure of the core of the planar waveguide and begins to propagate in it (see Fig. 19 and Fig. 20) . There is also a "gap" between the core and the prism, which is not shown in the figures. The gap in the study was a layer of an applied immersion liquid ( $n=1.515$ ).

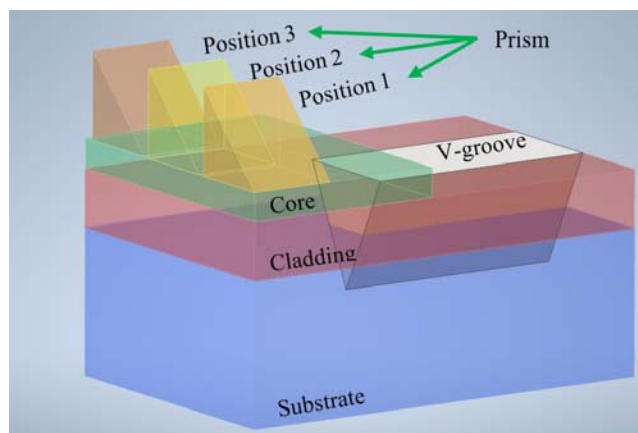


Fig. 19. Schematic of light coupling into the core of a planar waveguide using the prismatic method - 3D drawing

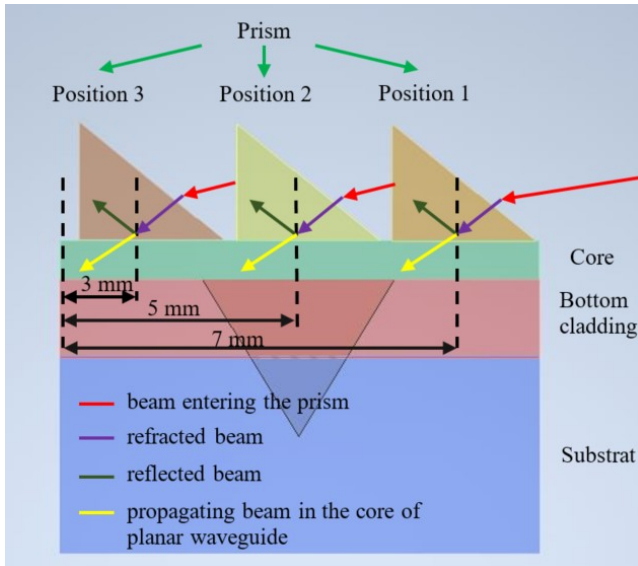


Fig. 20. Schematic of light coupling into the core of a planar waveguide using the prismatic method - 2D drawing

Measurements of the optical power propagated on the longer and shorter sections made it possible to determine the input and output optical power. Taking the optical power propagated on the shorter section of the planar waveguide as input and on the longer section as output, it is possible to determine the attenuation coefficient of the structure (4)[17]:

$$(4) \quad \alpha = \frac{10}{L_1 - L_2} \log \left( \frac{P_{L1}}{P_{L2}} \right) \left[ \frac{dB}{cm} \right]$$

where:  $L_1$ - longer fiber propagation section,  $L_2$ - shorter fiber propagation section,  $P_{L1}$ - output optical power on the longer fiber section,  $P_{L2}$ - output optical power on the shorter fiber section.

Before the experiment, the critical angles ( $\theta_c$ ) (5) were calculated between the core and upper cladding and the core and lower cladding. This action aimed to check for which propagation conditions would be observed for the occurrence of the total internal reflection phenomenon.

$$(5) \quad \theta_c = \arcsin \left( \frac{n_{cladding}}{n_{core}} \right)$$

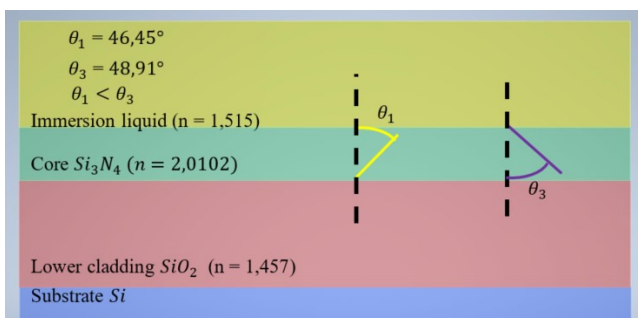


Fig. 21. Scheme of boundary angles for situations where the upper cladding is an immersion liquid - the drawing is not to scale

Using an immersion liquid - along the entire length of the planar waveguide (as the top cladding) - it was possible to couple the laser light beam into the planar waveguide. It enabled better contact between the prism and the planar optical fiber, as well as obtaining similar values of the critical angles between the core and the bottom cladding and the core and the top cladding (see Fig. 21). The dependence of the output optical power on the input optical

power was measured. The input optical power was taken as the total power propagated at the end of a fiber optic fiber - a pigtail - connected to a laser diode emitting a light beam with a wavelength of 635 nm. The designed optical table made it possible to make measurements not only for the lengths of structures defined by the construction of the planar waveguide but also for values falling between them. From the measurements of the dependence of the output optical power on the input, it can be seen that as the propagation length of the light beam in the planar waveguide increases, the power measured at the output decreases (see Fig. 22). It can be concluded that the measurements were performed correctly according to the classical definition of absorption, where the optical power decreases exponentially (see Fig. 23)

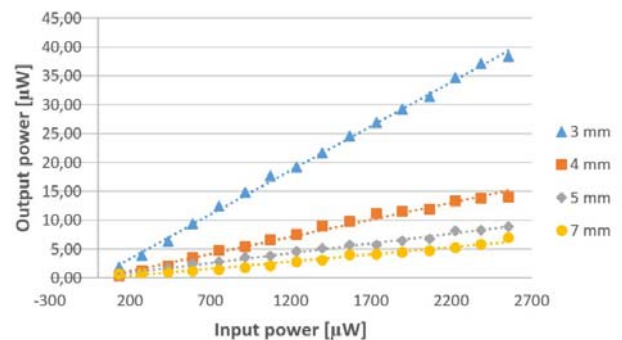


Fig. 22. Diagram showing output and input optical power values for planar waveguide - prismatic method

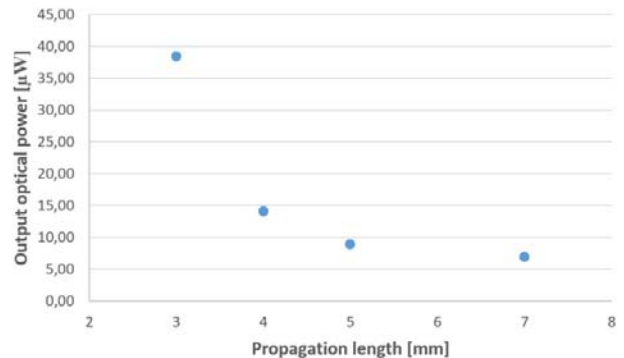


Fig. 23. A graph of the dependence of the output power on the propagation distance in a planar waveguide for the highest input power

## Discussion and conclusions

The purpose of the research was to study and verify the technologies that allow the coupling of light into optical planar waveguides. This paper presents two methods of coupling laser light into a planar waveguide: an end method and a prism method. The end method was carried out using a stepper motor for positioning the optical fiber with respect to the optical planar waveguide, while also using a V-groove.

To summarize the end method experiment using the motor stepper, it should be considered that this is a very time-consuming method due to the need to position the optical fibers relative to each other. The difficulty we also encountered was introducing enough power so that the light did not propagate above the core since only approximately 1% of the power from the optical fiber was transduced from the surface of the optical fiber to the planar waveguide. To improve the power using this method, equipment with even smaller travel steps would be necessary.

Therefore, the end coupling method using a V-groove is a good solution for integrated optics, as the V-groove avoids the long-term positioning requirement of the optical



fiber faces relative to each other and makes the system independent of the accuracy of the positioning instruments. Regarding the etching of the end surface of the groove, a much faster method is to use a femtosecond laser. For this end couple method to be effective, first, it is necessary to select an optical fiber core material where there will be a smaller difference in the refractive index of the optical fiber core. Second, to solve the problem of light leakage over the fiber core, a bent strip fiber can be produced. Future research should also develop a method that allows an optical fiber to be mounted in a V-groove in a repetitive manner so that the face of the optical fiber always contacts the face of the planar optical waveguide.

The prismatic method has proven to be the most effective method for coupling but also for decoupling from the planar optical waveguides. The experimental results show that this material has high attenuation, and the optical power decreases more than five times over a distance of 4 mm. The obtained experimental results clearly show the significant potential of this method. It can and should be used for the coupling and decoupling the light into and out of the optical planar waveguides in optical biosensors. The higher efficiency will be obtained by proper selection of the materials forming the waveguide and by optimization of the deposition technology, which should lead e.g. to lower material attenuation.

The experimental results demonstrated in this article show the importance of coupling and decoupling issues in integrated optical biosensors and photonic integrated circuits. The presented results provide a guideline for other groups working on integrated optics and biosensing.

**Acknowledgments** We would like to thank Bartosz Pruchnik for the design of the masks used for the fabrication of the optical planar waveguides.

**Authors:** Dr. Urszula Nawrot, Department of Nanometrology, Faculty of Electronics, Photonics and Microsystem, Wrocław University of Science and Technology, Janiszewskiego 11/17, 50-372 Wrocław, E-mail: [u.nawrot@pwr.edu.pl](mailto:u.nawrot@pwr.edu.pl), inż. Mikołaj Demuth, Department of Nanometrology, Faculty of Electronics, Photonics and Microsystem, Wrocław University of Science and Technology, Janiszewskiego 11/17, 50-372 Wrocław, E-mail: [235292@student.pwr.edu.pl](mailto:235292@student.pwr.edu.pl), dr. Andrzej Sierakowski, Institute of Microelectronics and Photonics, Łukasiewicz Research Network, Lotników 32/46, 02-668 Warsaw, E-mail: [andrzej.sierakowski@imif.lukasiewicz.gov.pl](mailto:andrzej.sierakowski@imif.lukasiewicz.gov.pl), mgr inż. Ewelina Gacka, Department of Nanometrology, Faculty of Electronics, Photonics and Microsystem, Wrocław University of Science and Technology, Janiszewskiego 11/17, 50-372 Wrocław, E-mail: [ewelina.gacka@pwr.edu.pl](mailto:ewelina.gacka@pwr.edu.pl), mgr inż. Krzysztof Pałka, Nanostructure Science and Technology Institute, Bierutowska 57-59, Building 17, 51-317 Wrocław, E-mail: [krzysztof.palka@nanores.pl](mailto:krzysztof.palka@nanores.pl), prof. dr hab. Teodor Gotszalk, Department of Nanometrology, Faculty of Electronics, Photonics and Microsystem, Wrocław

University of Science and Technology, Janiszewskiego 11/17, 50-372 Wrocław, E-mail: [teodor.gotszalk@pwr.edu.pl](mailto:teodor.gotszalk@pwr.edu.pl)

## REFERENCES

- [1] Pollock C., Lipson M., Integrated Photonics, *Springer Science*, Chapter 3 (2003), 43-67
- [2] Watanabe K., Kurata Y., Hiraki T., Nish H., Recent Progress in Optical Waveguide Technologies Enabling Integration of High-density Compact Photonics, *NTT Technical Review*, 15 (2017) No. 1
- [3] Chen Ch., Wang J., Optical biosensors: an exhaustive and comprehensive review, *Analyst*, 145 (2020), 1605
- [4] Peng C., Yang C., Zhao H., Liang L., Zheng C., Chen C., Qin L., Tang H., Optical Waveguide Refractive Index Sensor for Biochemical Sensing, *Applied Sciences*, 13 (2023), No. 6, 3829
- [5] Lavers C., Itoh K., Wu S., Murabayashi M., Mauchline I., Stewart G., Stout T., Planar optical waveguides for sensing applications, *Sensors and Actuators B: Chemical*, 69 (2000), 1-2, 85-9
- [6] Chang G., Barshilia D. Chau L., Low-cost planar waveguide-based optofluidic sensor for real-time refractive index sensing, *Optics Express*, 28 (2020), 19
- [7] Gyeongho S., Seungjun H., Jongwoo P., Kyungmok K., Kyoungsik Y., High-efficiency broadband light coupling between optical fibers and photonic integrated circuits *Nanophotonics*, 7 (2018) no. 12, 1845-1864
- [8] Pustelny T., Struk P., Numerical analyses of optical couplers for planar waveguides, *Opto-Electronics Review*, 20 (2012) no. 3, 201-206
- [9] Krasieński P., Planar Optical Waveguide Sensor Structures with Grating Couplers, *Proceedings of the III National Conference on Nanotechnology*, 116 (2009), 30-32
- [10] Duarte, L., Hernandez, A., Duarte, C., Barêa, L. (2021). Sensitivity improvement in Si<sub>3</sub>N<sub>4</sub> tapered waveguides for compact refractive index sensors, *Optics Communications*, 499 (2021) 127265
- [11] Saleh B., Teich M., Fundamentals of Photonics, *Wiley*, Chapter 9 (2019), 821- 824
- [12] Miller S., Kaminow I., Optical Fiber Telecommunications II, Academic Press Chapter 14 (1988), 589
- [13] "refractive index info," [Online]. Available: <https://refractiveindex.info/?shelf=main&book=SiO2&page=Maltson>. [Access date: June 20, 2023].
- [14] Utke I., Michler J., Winkler R., Plank H., Mechanical Properties of 3D Nanostructures Obtained by Focused Electron/Ion Beam-Induced Deposition: A Review, *Micromachines*, 11 (2020), 397
- [15] Kunicki P., Angelov T., Ivanov T., Gotszalk T., Rangelow I., Sensitivity Improvement to Active Piezoresistive AFM Probes Using Focused Ion Beam Processing, *Sensors*, 19 (2019), 4429
- [16] Llobet J., Gerbolés M., Sansa M., Bausells J., Borrísé X., Pérez-Murano F., Fabrication of functional electromechanical nanowire resonators by focused ion beam implantation, *Journal of Micro/Nanolithography, MEMS, and MOEMS* 14(2015), 031207
- [17] Hecht J., Understanding Fiber Optics, Laser Light Press, Chapter 5 (2016, 93-99